

A New Versatile Class of Hetero-tetra-metallic Assemblies: Highlighting Single-molecule Magnet Behaviour

Nathalie Bridonneau, Lise-Marie Chamoreau, Philippe P. Lainé,
Wolfgang Wernsdorfer and Valérie Marvaud*.

Supplementary Information

{[((valen)Cu)Tb(OH₂)₂(μMo(CN)₈)]₂•2[Ni(tpy)₂] }(ClO₄)₂ noted (1)

{[((valen)Cu)Tb(OH₂)₂(μMo(CN)₈)]₂•2[Ru(tpy)₂] } (NO₃)₂ noted (2)

{[((valen)Cu)Tb(OH₂)₂(μMo(CN)₈)]₂•2[Os(tpy)₂] } (NO₃)₂ noted (3)

{[((valen)Cu)Tb(OH₂)₂(μW(CN)₈)]₂•2[Ni(tpy)₂] }(ClO₄)₂ noted (4)

{[((valen)Cu)Tb(OH₂)₂(μW(CN)₈)]₂•2[Ru(tpy)₂] } (NO₃)₂ noted (5)

{[((valen)Cu)Tb(OH₂)₂(μW(CN)₈)]₂•2[Os(tpy)₂] } (NO₃)₂ noted (6)

Note : The related compounds CuGdMo-Ni, NiTbMo-Ni, NiGdMo-Ni as well as tungsten analogues will be fully described elsewhere.

Experimental Section

Crystallographic data for (1), (2), (4) and (6)

Magnetic Properties for (1), (2), (3), (4), (5) and (6)

Preparation of hetero-tetrametallic compounds:

The ligand valen (*N,N'*-bis(3-methoxysalicylidene)ethylenediamine), noted L, was synthesized by reacting one equivalent of ethylenediamine with two equivalents of o-vanillin in ethanol. The bimetallic building block $[\text{CuLTb}](\text{NO}_3)_3$ was synthesized according to the protocol of the literature.^{S1}

Caution! Cyanides are very toxic and must be handled with carefulness.

Although no problem was encountered in this work, perchlorate complexes are potentially explosive and should be handled with great care.

Complex 1: $\{[(\text{valen})\text{Cu}\text{Tb}(\text{OH}_2)_2(\mu\text{Mo}(\text{CN})_8)]_2 \bullet 2[\text{Ni}(\text{tpy})_2]\}(\text{ClO}_4)_2$

$[\text{Mo}(\text{CN})_8]\text{K}_4\cdot 2\text{H}_2\text{O}$ (0.030 g, 0.06 mmol) in 5mL of water was carefully added to a solution of $[\text{Cu-valen-Tb}](\text{NO}_3)_3$; 0.047 g, 0.06 mmol) in water/acetonitrile (1: 2, 15 mL). The mixture was stirred for 5 minutes before adding a solution of $[\text{Ni}(\text{terpy})_2](\text{ClO}_4)_2$ previously prepared in the same solvent from $[\text{Ni}(\text{ClO}_4)_2]\cdot 6\text{H}_2\text{O}$ (0.022 g, 0.06 mmol) and 2, 2':6', 2''-Terpyridine (0.028 g, 0.12 mmol). Slow evaporation in the dark of the brown solution afforded red crystals after a few days.

Yield = 46 %; IR (KBr): 2151, 2146, 2118, 2107, 1631, 1602, 1474, 1450, 1388, 1287, 1221, 1100, 1079, 778, 739, 641. Anal Calc for Mo₂ Cu₂ Tb₂ Ni₂ C₁₁₂ H₁₃₆ N₃₂ O₄₄ Cl₂: C 38.17, H 4.00, N 12.72, Mo 5.44, Cu 3.61, Tb 9.02, Ni 3.33, Cl 2.01. Found: C 39.77, H 3.77, N 13.73, Mo 5.46, Cu 3.65, Tb 8.55, Ni 3.39, Cl 1.57.

Complex 2: $\{[(\text{valen})\text{Cu}\text{Tb}(\text{OH}_2)_2(\mu\text{Mo}(\text{CN})_8)]_2 \bullet 2[\text{Ru}(\text{tpy})_2]\}(\text{NO}_3)_2$

Similar procedure has been used for the ruthenium complex, starting with $[\text{Ru}(\text{terpy})_2](\text{PF}_6)_2$. Yield = 48 %; IR (KBr): 2152, 2146, 2118, 2107, 1633, 1602, 1474, 1450, 1389, 1289, 1221, 1100, 1079, 838, 772, 739.

Complex 3: $\{[(\text{valen})\text{Cu}\text{Tb}(\text{OH}_2)_2(\mu\text{Mo}(\text{CN})_8)]_2 \bullet 2[\text{Os}(\text{tpy})_2]\}(\text{NO}_3)_2$

Similar procedure has been used for the osmium complex, starting with $[\text{Os}(\text{terpy})_2](\text{PF}_6)_2$. Yield = 17 %; IR (KBr): 2151, 2141, 2114, 2104, 1631, 1602, 1474, 1450, 1389, 1283, 1222, 1100, 1079, 778, 738. Anal Calc for Mo₂ Cu₂ Tb₂ Os₂ C₁₁₂ H₁₃₆ N₃₂ O₄₄ Cl₂: C 36.24, H 3.80, N 12.03, Mo 5.16, Cu 3.42, Tb 8.56. Found: C 36.66, H 3.29, N 10.94, Mo 4.20, Cu 3.89, Tb 7.35.

Complex 4 : {[((valen)Cu)Tb(OH₂)₂(μW(CN)₈)]₂•2[Ni(tpy)₂] } (ClO₄)₂

Complex 4 was obtained using the same experimental procedure, with [W(CN)₈]K₄.2H₂O (0.035 g, 0.06 mmol). Slow evaporation in the dark of the brown solution afforded brown crystals after a few days.

Yield = 15 %; IR (KBr): 2151, 2141, 2118, 2107, 1631, 1604, 1475, 1449, 1391, 1289, 1222, 1173, 1102, 1066, 773, 742, 648. Anal Calc for W₂ Cu₂ Tb₂ Ni₂ C₁₁₂ H₁₃₆ N₃₂ O₄₄ Cl₂ : C 36.96, H 3.81, N 12.11, W 9.94, Cu 3.44, Tb 8.59, Ni 3.17, Cl 1.92. Found: C 38.06, H 3.47, N 12.72, W 9.02, Cu 3.25, Tb 8.00, Ni 3.34, Cl 1.99.

Complex 5 : {[((valen)Cu)Tb(OH₂)₂(μW(CN)₈)]₂•2[Ru(tpy)₂] } (NO₃)₂

Similar procedure has been used for the ruthenium complex, starting with [Ru(terpy)₂](PF₆)₂. Yield = 35 %; IR (KBr): 3430, 2152, 2142, 2116, 2105, 1630, 1450, 1380, 1285, 1220, 780, 740. Anal Calc for W₂ Cu₂ Tb₂ Ru₂ C₁₁₂ H₁₃₆ N₃₂ O₄₄ Cl₂ : C 36.26, H 3.80, N 12.14, W 9.91, Cu 3.42, Tb 8.57, Ru 5.45. Found: C 36.11, H 3.56, N 12.39, W 7.02, Cu 1.98, Tb 3.80, Ru 7.47.

Complex 6 : {[((valen)Cu)Tb(OH₂)₂(μW(CN)₈)]₂•2[Os(tpy)₂] } (NO₃)₂

Similar procedure has been used for the ruthenium complex, starting with [Os(terpy)₂](PF₆)₂. Yield = 14 %; IR (KBr): 3430, 2151, 2141, 2114, 2104, 1630, 1450, 1380, 1285, 1220, 1070, 1030, 780, 740. Anal Calc for W₂ Cu₂ Tb₂ Os₂ C₁₁₂ H₈₀ N₃₂ O₁₆ Cl₂ : C 34.60, H 3.63, N 11.49, W 9.46, Cu 3.27, Tb 8.17. Found: C 33.84, H 2.88, N 11.09, W 9.06, Cu 2.74, Tb 7.11.

Physical Measurements.

IR spectra were obtained between 4000 and 250 cm⁻¹ on a Bio-Rad FTS 165 FT-IR spectrometer on KBr pellets. DC magnetic susceptibility measurements were carried out on a Quantum Design MPMS SQUID susceptometer equipped with a 5 T magnet and operating in the range of temperature from 2 to 400 K. The powdered samples (10±50mg) were placed in a diamagnetic sample holder and the measurements realised in a 1000 Oe applied field using the extraction technique. Before analysis, the experimental susceptibility was corrected from diamagnetism using Pascal constants and from temperature independent paramagnetism (TIP)

of the transition metals. AC susceptibility measurements were performed using an oscillating field of 1 Oe and AC frequencies ranging from 10 to 9007 Hz.

Infrared Spectroscopy of $\{[(\text{valen})\text{Cu}]\text{Tb}(\text{OH}_2)_2(\mu\text{Mo}(\text{CN})_8)]_2 \bullet 2[\text{Ni}(\text{tpy})_2]\}(\text{ClO}_4)_2$ complex (**1**)

The IR spectrum shows several large bands in the cyanide region 2000-2200 cm^{-1} located at 2108, 2118 cm^{-1} and shoulders at 2147 and 2153 cm^{-1} . These bands can be ascribed to the envelope of free cyanide Mo-C≡N and bridged cyanide Mo-C≡N-M respectively. The bands of the valen ligand are found at 1220, 1290 and 1630 cm^{-1} ($\nu(\text{C}=\text{N})$ stretching). Perchlorate ions appear at 1091 and 647 cm^{-1} .

Similar assignment might be done for the other compounds:

2152, 2146, 2118, 2107 for (**2**)

2152, 2145, 2118, 2107 for (**3**)

2151, 2141, 2118, 2107 for (**4**)

2152, 2142, 2116, 2105 for (**5**)

2151, 2141, 2114, 2104 for (**6**)

X-Ray Crystallography

Suitable crystals for X-ray crystallography were directly obtained from the reaction medium. A single crystal of the compounds was selected rapidly, mounted onto a glass fiber, and transferred in a cold nitrogen gas stream. Intensity data were collected with a Bruker-Nonius Kappa-CCD with graphite-monochromated Mo-K α radiation ($\lambda = 0.71073 \text{ \AA}$). Unit-cell parameters determination, data collection strategy and integration were carried out with the Nonius EVAL-14 suite of programs.³³ The structure was solved by direct methods using the SIR-92 program³⁴ and refined anisotropically by full-matrix least-squares methods using the SHELXL-97 software package (G. M. Sheldrick, University of Göttingen, Germany, 1997).

Single Crystal X-Ray Structure of $\{[(\text{valen})\text{Cu}]\text{Tb}(\text{OH}_2)_2(\mu\text{Mo}(\text{CN})_8)\}_2 \bullet 2[\text{Ni}(\text{tpy})_2]\}(\text{ClO}_4)_2$ (1)

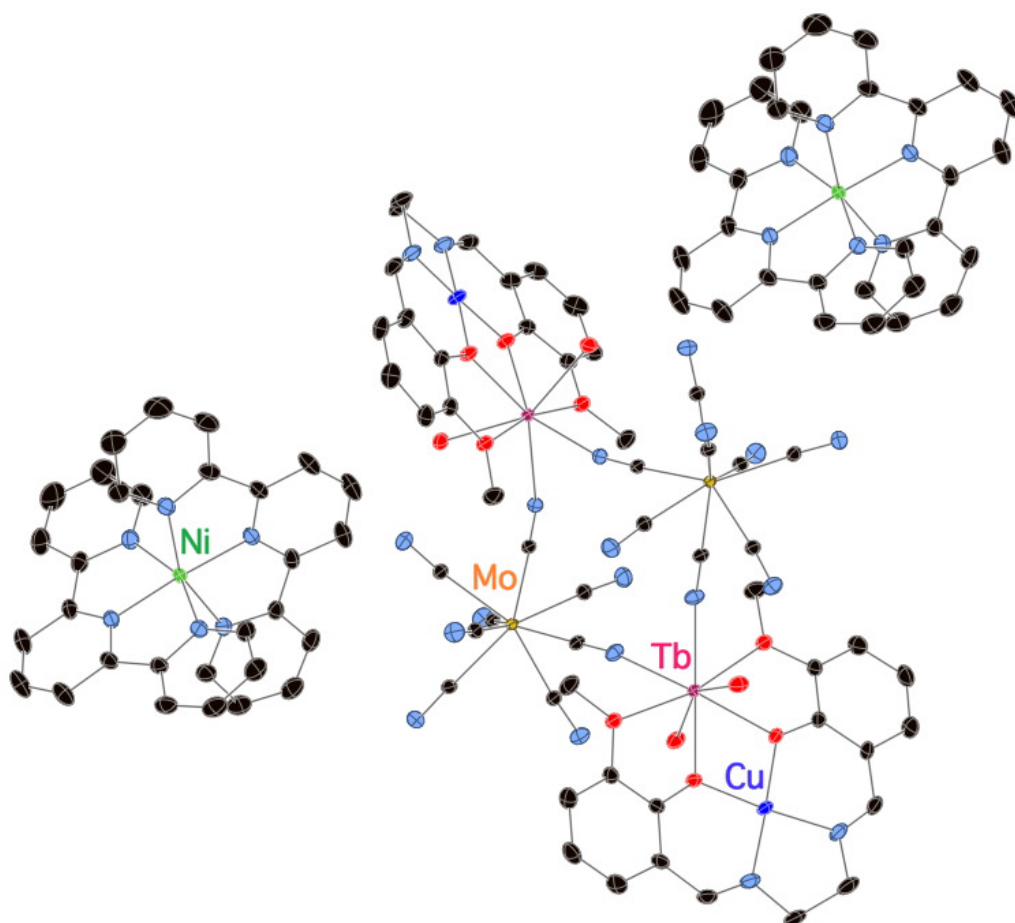


Figure S1. Ortep representation of the X-ray crystal structure of (1)
(thermal ellipsoids set at the 30 % probability level)

Single Crystal X-Ray Structure of
 $\{[(\text{valen})\text{Cu}]\text{Tb}(\text{OH}_2)_2(\mu\text{Mo}(\text{CN})_8)]_2 \bullet 2[\text{Ru}(\text{tpy})_2]\}\text{(NO}_3)_2$ (2)

The X-ray structure reveals that (2) is isostructural to the Nickel equivalent. The compound crystallizes in an orthorhombic system with an Fddd space group. The cell parameters for (2) are $a = 22.9246(7)$ Å, $b = 29.8958(9)$ Å, $c = 41.9514(14)$ Å, the cell volume is 28751.4(16) Å³. The Ru-N distances are equal to 1.989, 2.077 and 2.086 Å while the angles range from 78.28 to 104.35 °.

The coordination spheres of the molybdenum, the terbium and the copper are identical to the nickel analogue.

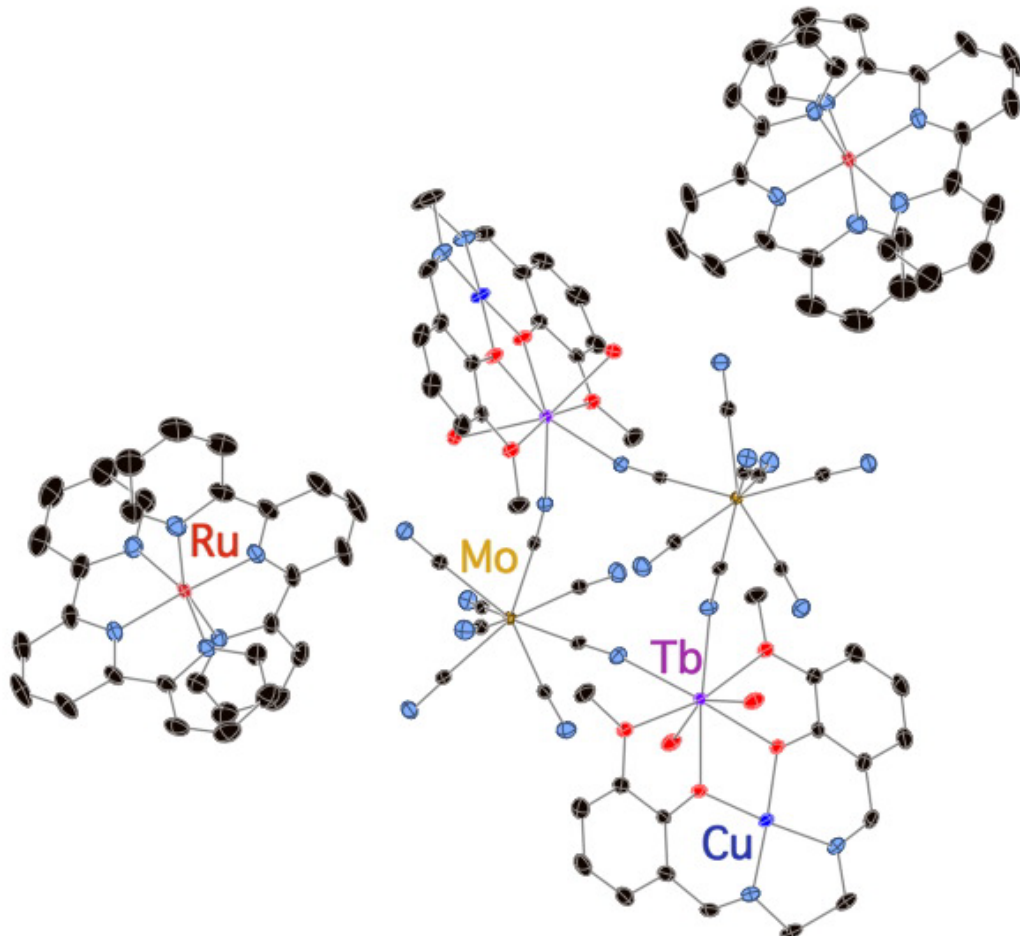


Figure S2. Ortep representation of the X-ray crystal structure of (2)
(thermal ellipsoids set at the 30 % probability level)

Single Crystal X-Ray Structure of



The X-ray structure reveals that (4) is isostructural to the molybdenum equivalent. The compound crystallizes in an orthorhombic system with an Fddd space group. The cell parameters for (6) are $a = 23.0007(7)$ Å, $b = 29.7883(9)$ Å, $c = 42.1077(12)$ Å, the cell volume is $28\ 850.2(15)$ Å³. The W-C distances are equal to 2.133 (bridge), 2.165, 2.169 and 2.170 Å while the angles range from 73.38 to 80.57 °.

The coordination spheres of the tungsten, the terbium and the copper are identical to the molybdenum analogue.

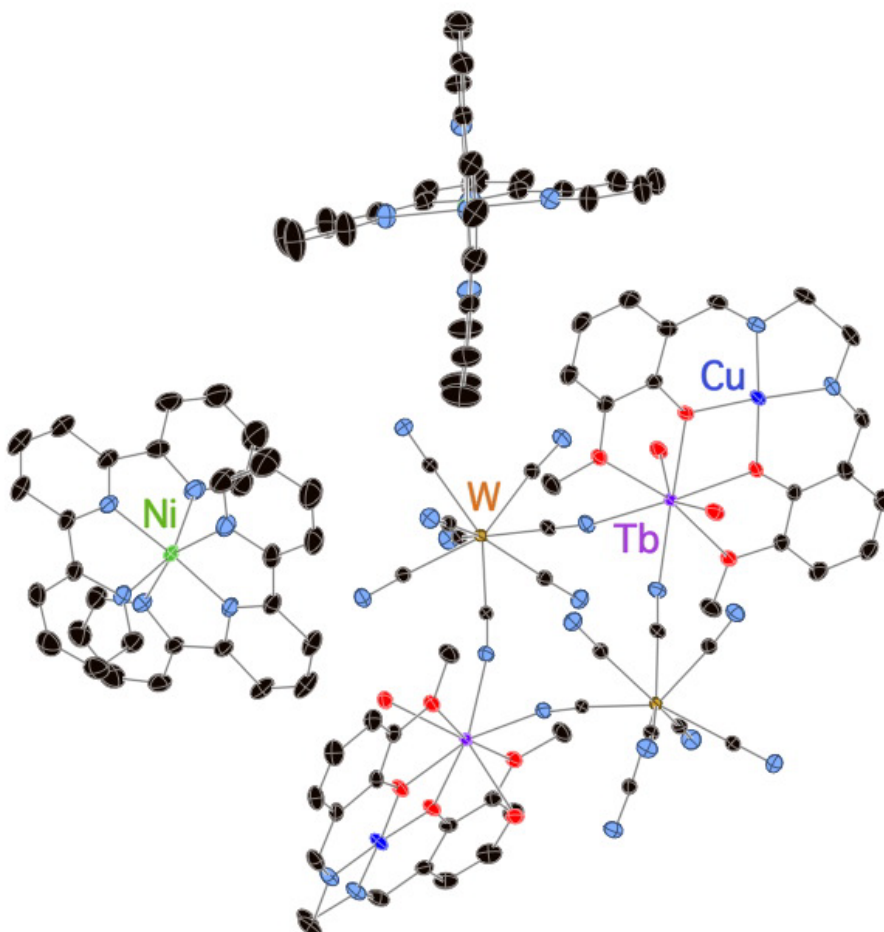


Figure S3. Ortep representation of the X-ray crystal structure of (4)
(thermal ellipsoids set at the 30 % probability level)

Single Crystal X-Ray Structure of



The X-ray structure reveals that (6) is isostructural to the Nickel equivalent. The compound crystallizes in an orthorhombic system with an Fddd space group. The cell parameters for (6) are $a = 22.8937 \text{ \AA}$, $b = 29.8563 \text{ \AA}$, $c = 41.8842 \text{ \AA}$, the cell volume is 28626.7 \AA^3 .

The Os-N distances are equal to 1.990, 2.050 and 2.067 \AA while the angles range from 79.29 to 103.07 $^\circ$.

The coordination spheres of the molybdenum, the terbium and the copper are identical to the nickel analogue.

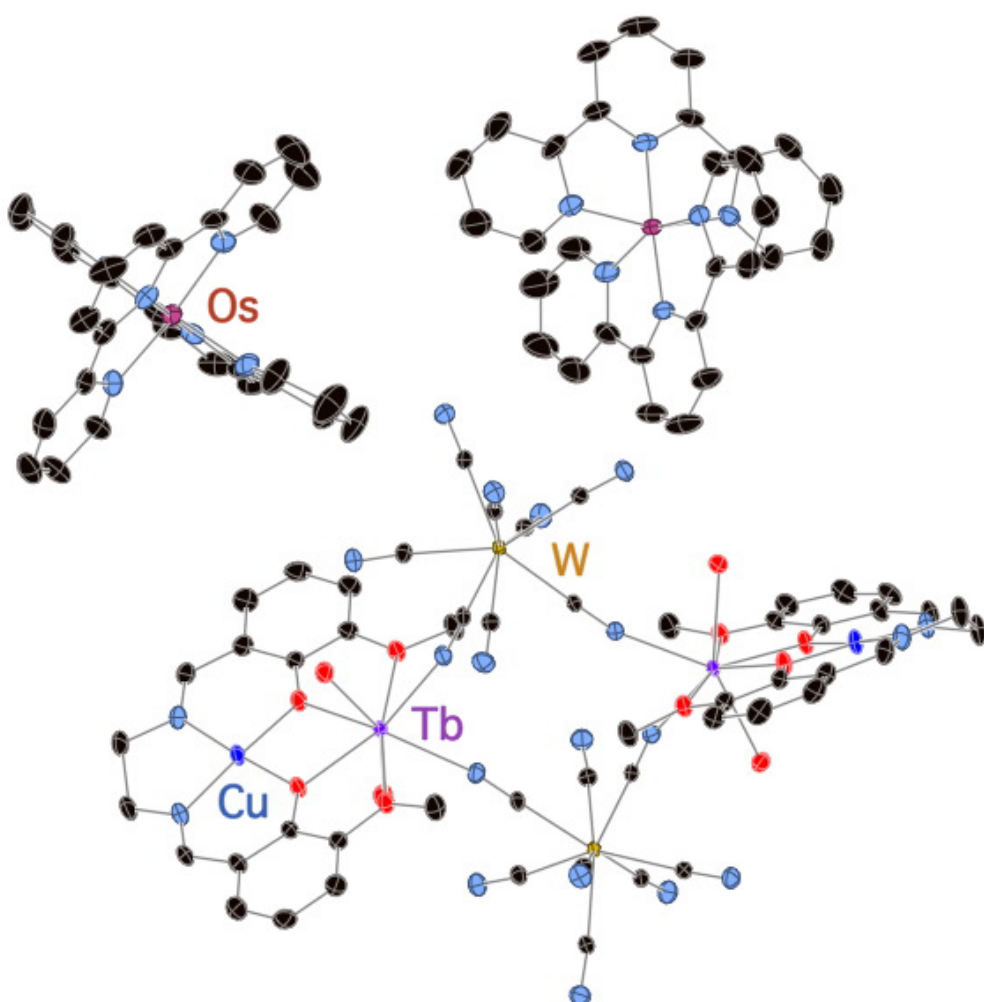


Figure S4. Ortep representation of the X-ray crystal structure of (6)
(thermal ellipsoids set at the 30 % probability level)

Crystal data and structure refinement for (1)



Identification code	nb3-195
Empirical formula	C112 H136 Cl2 Cu2 Mo2 N32 Ni2 O44 Tb2
Formula weight	3459.65
Temperature	200(2) K
Wavelength	0.71073 Å
Crystal system	Orthorhombic
Space group	F d d
Unit cell dimensions	$a = 23.0051(4)$ Å $\alpha = 90^\circ$. $b = 29.8285(6)$ Å $\beta = 90^\circ$. $c = 42.2334(8)$ Å $\gamma = 90^\circ$.
Volume	28980.9(9) Å ³
Z	8
Density (calculated)	1.586 Mg/m ³
Absorption coefficient	1.797 mm ⁻¹
F(000)	13968
Crystal size	0.44 x 0.31 x 0.22 mm ³
Theta range for data collection	1.83 to 32.02° .
Index ranges	-34≤h≤34, -28≤k≤44, -54≤l≤62
Reflections collected	83991
Independent reflections	12598 [R(int) = 0.0208]
Completeness to theta = 32.02°	99.9 %
Absorption correction	Semi-empirical from equivalents
Max. and min. transmission	0.9481 and 0.9302
Refinement method	Full-matrix least-squares on F ²
Data / restraints / parameters	12598 / 2 / 425
Goodness-of-fit on F ²	1.089
Final R indices [I>2sigma(I)]	R1 = 0.0431, wR2 = 0.1210
R indices (all data)	R1 = 0.0607, wR2 = 0.1396
Largest diff. peak and hole	3.451 and -1.563 e.Å ⁻³

Crystal data and structure refinement for (2)



Identification code	nb4-90	
Empirical formula	C112 H144 Cl0 Cu2 Mo2 N34 O46 Ru2 Tb2	
Formula weight	3541.55	
Temperature	200(2) K	
Wavelength	0.71073 Å	
Crystal system	Orthorhombic	
Space group	F d d d	
Unit cell dimensions	$a = 22.9246(7)$ Å	$\alpha = 90^\circ$.
	$b = 29.8958(9)$ Å	$\beta = 90^\circ$.
	$c = 41.9514(14)$ Å	$\gamma = 90^\circ$.
Volume	28751.4(16) Å ³	
Z	8	
Density (calculated)	1.636 Mg/m ³	
Absorption coefficient	1.725 mm ⁻¹	
F(000)	14256	
Crystal size	0.22 x 0.11 x 0.11 mm ³	
Theta range for data collection	1.94 to 29.97° .	
Index ranges	-31≤h≤31, -41≤k≤22, -58≤l≤58	
Reflections collected	55017	
Independent reflections	10367 [R(int) = 0.0334]	
Completeness to theta = 29.97°	98.9 %	
Absorption correction	Semi-empirical from equivalents	
Max. and min. transmission	0.746 and 0.672	
Refinement method	Full-matrix least-squares on F ²	
Data / restraints / parameters	10367 / 8 / 441	
Goodness-of-fit on F ²	1.032	
Final R indices [I>2sigma(I)]	R1 = 0.0383, wR2 = 0.0934	
R indices (all data)	R1 = 0.0618, wR2 = 0.1061	
Largest diff. peak and hole	1.592 and -1.065 e.Å ⁻³	

Crystal data and structure refinement for (4)



Identification code	nb4-11
Empirical formula	C112 H136 Cl2 Cu2 N32 Ni2 O44 Tb2 W2
Formula weight	3635.47
Temperature	200(2) K
Wavelength	0.71073 Å
Crystal system	Orthorhombic
Space group	F d d d
Unit cell dimensions	a = 23.0007(7) Å $\alpha = 90^\circ$. b = 29.7883(9) Å $\beta = 90^\circ$. c = 42.1077(12) Å $\gamma = 90^\circ$.
Volume	28850.2(15) Å ³
Z	8
Density (calculated)	1.674 Mg/m ³
Absorption coefficient	3.225 mm ⁻¹
F(000)	14480
Crystal size	0.22 x 0.18 x 0.11 mm ³
Theta range for data collection	1.67 to 32.02° .
Index ranges	-21≤h≤34, -44≤k≤44, -62≤l≤46
Reflections collected	85990
Independent reflections	12546 [R(int) = 0.0254]
Completeness to theta = 32.02°	99.8 %
Absorption correction	Semi-empirical from equivalents
Max. and min. transmission	0.746 and 0.672
Refinement method	Full-matrix least-squares on F ²
Data / restraints / parameters	12546 / 1 / 453
Goodness-of-fit on F ²	0.992
Final R indices [I>2sigma(I)]	R1 = 0.0315, wR2 = 0.0846
R indices (all data)	R1 = 0.0549, wR2 = 0.1038
Largest diff. peak and hole	1.947 and -1.723 e.Å ⁻³

Crystal data and structure refinement for (6)



Identification code	nb6-148		
Empirical formula	C112 H140 Cu2 N34 O40 Os2 Tb2 W2		
Formula weight	3795.75		
Temperature	200(1) K		
Wavelength	0.71073 \approx		
Crystal system	Orthorhombic		
Space group	F d d d		
Unit cell dimensions	$a = 22.8937(7)$ Å	$\alpha = 90^\circ$.
	$b = 29.8563(10)$ Å	$\beta = 90^\circ$.
	$c = 41.8842(13)$ Å	$\gamma = 90^\circ$.
Volume	28628.7(16) Å ³		
Z	8		
Density (calculated)	1.744 Mg/m ³		
Absorption coefficient	4.719 mm ⁻¹		
F(000)	14576		
Crystal size	0.3 x 0.25 x 0.2 mm ³		
Theta range for data collection	1.84 to 32.02 ∞ .		
Index ranges	-23 \leq h \leq 34, -44 \leq k \leq 37, -47 \leq l \leq 62		
Reflections collected	68209		
Independent reflections	12436 [R(int) = 0.0330]		
Completeness to theta = 32.02 $^\circ$	99.8 %		
Absorption correction	Semi-empirical from equivalents		
Max. and min. transmission	0.3385 and 0.2522		
Refinement method	Full-matrix least-squares on F ²		
Data / restraints / parameters	12436 / 7 / 453		
Goodness-of-fit on F ²	1.059		
Final R indices [I>2sigma(I)]	R1 = 0.0366, wR2 = 0.1012		
R indices (all data)	R1 = 0.0637, wR2 = 0.1226		
Largest diff. peak and hole	3.193 and -3.124 e.Å ⁻³		

Magnetic Properties

Magnetic Properties of $\{[(\text{valen})\text{Cu}]\text{Tb}(\text{OH}_2)_2(\mu\text{Mo}(\text{CN})_8)]_2 \bullet 2[\text{Ni}(\text{tpy})_2]\}(\text{ClO}_4)_2$ (1)

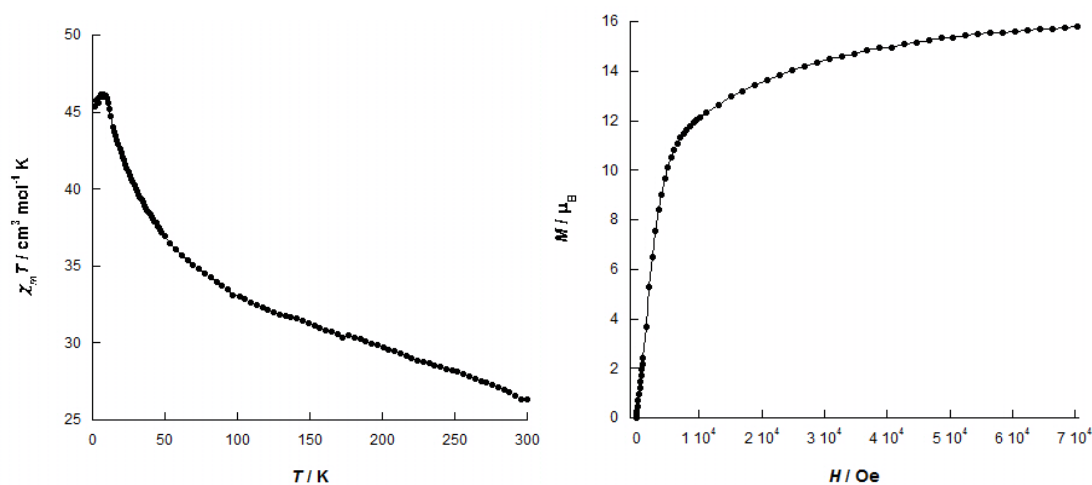


Figure S5: Variation of χT vs. T ($H=1000\text{G}$) and M vs. H at 2K for (1)

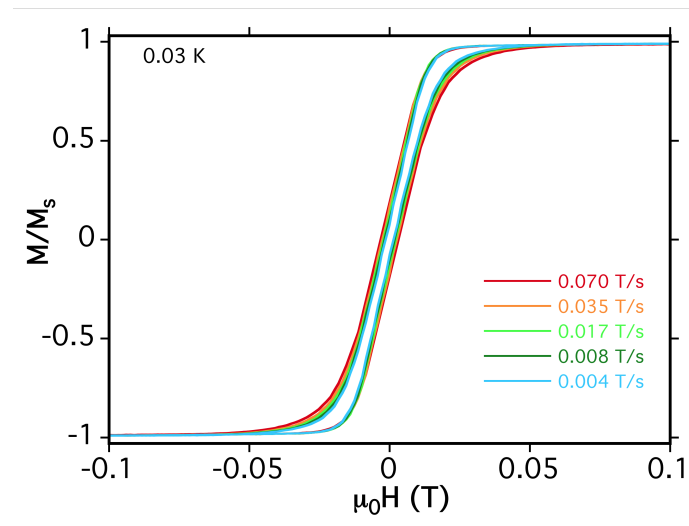


Figure S6: Hysteresis loop at 0.03 K

Magnetic Properties of $\{[(\text{valen})\text{Cu}]\text{Tb}(\text{OH}_2)_2(\mu\text{Mo}(\text{CN})_8)\}_2 \bullet 2[\text{Ru}(\text{tpy})_2]\}(\text{NO}_3)_2$ (2)

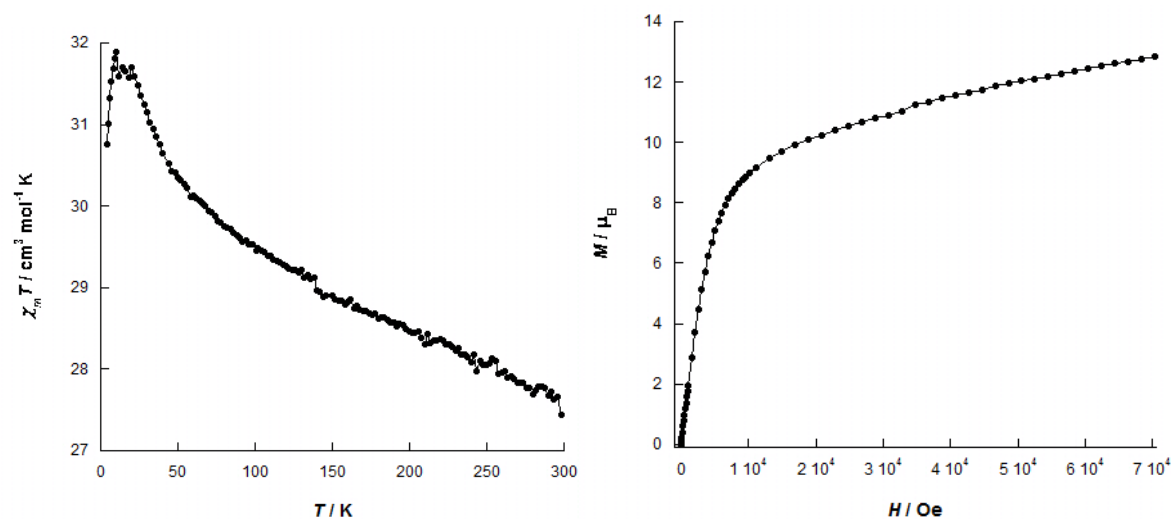


Figure S7: Variation of χT vs. T ($H=1000\text{G}$) and M vs. H at 2K for (2)

Magnetic Properties of $\{[(\text{valen})\text{Cu}]\text{Tb}(\text{OH}_2)_2(\mu\text{Mo}(\text{CN})_8)\}_2 \bullet 2[\text{Os}(\text{tpy})_2]\}(\text{NO}_3)_2$ (3)

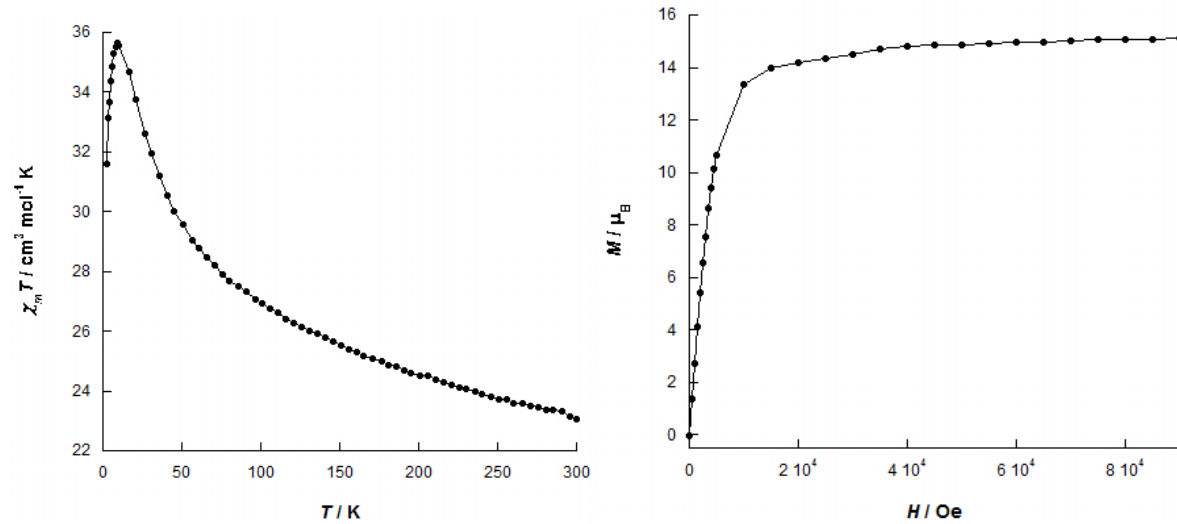


Figure S8: Variation of χT vs. T ($H=1000\text{G}$) and M vs. H at 2K for (3)

Magnetic Properties of $\{[(\text{valen})\text{Cu}]\text{Tb}(\text{OH}_2)_2(\mu\text{W}(\text{CN})_8)\}_2 \bullet 2[\text{Ni}(\text{tpy})_2]\}(\text{ClO}_4)_2$ (4)

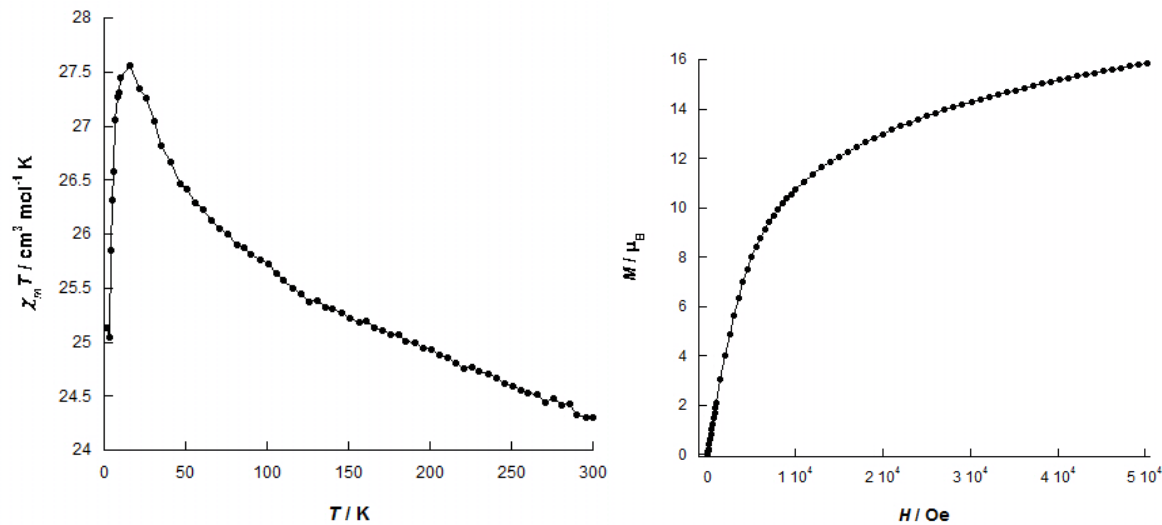


Figure S9: Variation of χT vs. T (H=1000G) and M vs. H at 2K for (4)

Magnetic Properties of $\{[(\text{valen})\text{Cu}]\text{Tb}(\text{OH}_2)_2(\mu\text{W}(\text{CN})_8)\}_2 \bullet 2[\text{Ru}(\text{tpy})_2]\}(\text{NO}_3)_2$ (5)

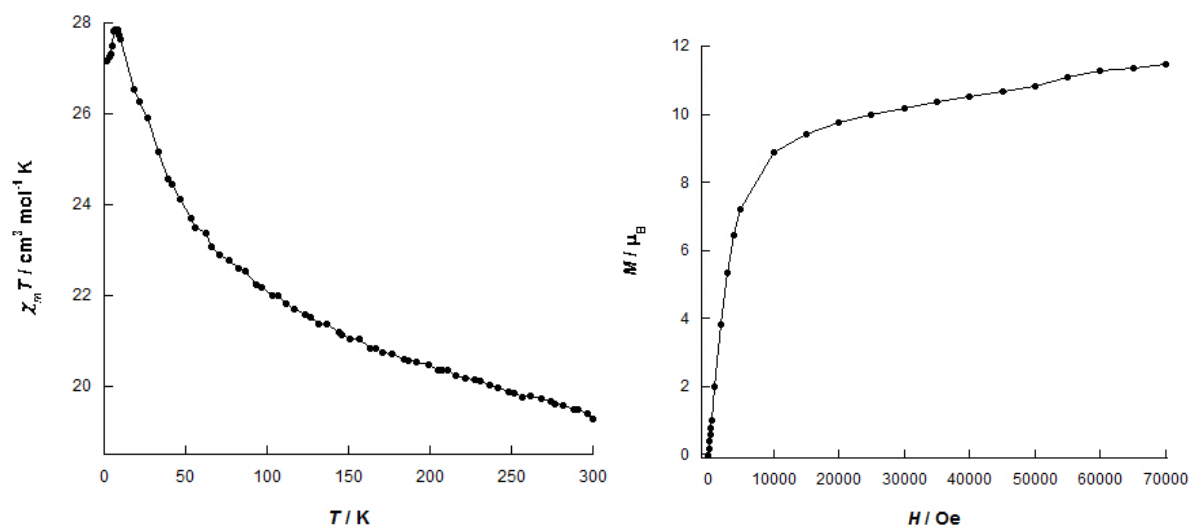


Figure S10: Variation of χT vs. T (H=1000G) and M vs. H at 2K for (5)

Magnetic Properties of $\{[(\text{valen})\text{Cu}]\text{Tb}(\text{OH}_2)_2(\mu\text{W}(\text{CN})_8)\}_2 \bullet 2[\text{Os}(\text{tpy})_2]\}(\text{NO}_3)_2$ (6)

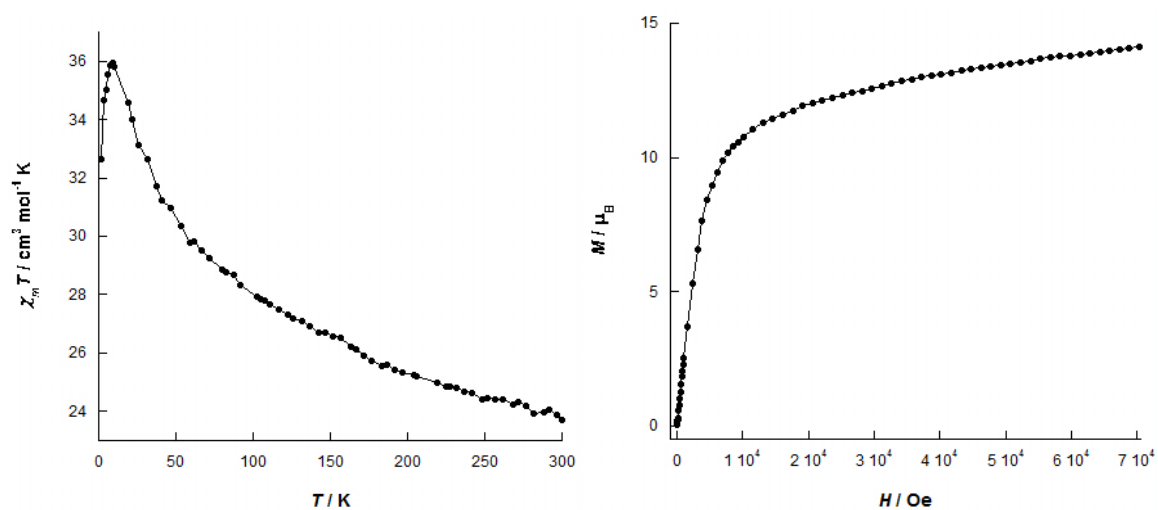


Figure S11: Variation of χT vs. T ($H=1000\text{G}$) and M vs. H at 2K for (6)

Photomagnetic studies

The photomagnetic experiments do not show any drastic change of the magnetic properties after irradiation with a lamp ($\lambda = 405 \text{ nm}$). Indeed, the X-ray structure shows clearly that the copper is not directly connected via the cyano-bridge to the molybdenum limiting the possibility of an electron transfer between these two metallic centers through the orbitals of the cyanide. However, it has been shown that for such systems, an outer-sphere electron transfer can occur.^{S2} One can also imagine, an electron transfer from the molybdenum to the copper via the semi-occupied orbitals of the terbium. More recently, we have also demonstrated the feasibility to stabilize Mo(IV) in a high spin configuration, but none of these effect has been observed in the present work and no long lived photo induced metastable state has been evidenced.

References :

- (S1) Costes, J.-P.; Dahan, F.; Dupuis, A.; Laurent, J. *Inorg Chem*, **1996**, *35*, 2400-2402.
(S2) Korzeniak, T.; Mathonière, C.; Kaiba, A.; Guionneau, P.; Koziel, M.; Sieklucka, B. *Inorg. Chim. Acta*, **2008**, *361*, 12-13, 3500-3504.